
Mathematical Population Studies: An International Journal of Mathematical Demography

Publication details, including instructions for authors and subscription information:
http://www.tandfonline.com/loi/gmps20

# A Discrete-Time Branching Process Model of Yeast Prion Curing Curves*

SUZANNE S. SINDI [a] & PETER OLOFSSON [b]

[a] School of Natural Sciences, University of California, Merced, California, USA

[b] Department of Mathematics, Trinity University, San Antonio, Texas, USA

Version of record first published: 27 Jan 2013.

To cite this article: SUZANNE S. SINDI & PETER OLOFSSON (2013): A Discrete-Time Branching Process Model of Yeast Prion Curing Curves*, Mathematical Population Studies: An International Journal of Mathematical Demography, 20:1, 1-13

To link to this article: http://dx.doi.org/10.1080/08898480.2013.748566

*Mathematical Population Studies*, 20:1–13, 2013

ISSN: 0889-8480 print/1547-724X online
DOI: 10.1080/08898480.2013.748566

Routledge
Taylor & Francis Group



# A DISCRETE-TIME BRANCHING PROCESS MODEL OF YEAST PRION CURING CURVES*

**Suzanne S. Sindi**
*School of Natural Sciences, University of California, Merced, California, USA*

**Peter Olofsson**
*Department of Mathematics, Trinity University, San Antonio, Texas, USA*

***The infectious agent of many neurodegenerative disorders is thought to be aggregates of prion protein, which are transmitted between cells. Recent work in yeast supports this hypothesis but also suggests that only aggregates below a critical size are transmitted efficiently. The total number of transmissible aggregates in a typical cell is a key determinant of strain infectivity.***

***In a discrete-time branching process model of a yeast colony with prions, prion aggregates increase in size according to a Poisson process and only aggregates below a threshold size are transmitted during cell division. The total number of cells with aggregates in a growing population of yeast is expressed.***

***Keywords***: branching process; curing curves; Poisson process; prion; yeast

## 1. INTRODUCTION

Transmission of an observable trait, or phenotype, need not involve changes to DNA. Heritable phenotypes are also passed on by a special class of proteins called prions. In mammals, the prion protein PrP has been implicated in a variety of neurodegenerative disorders such as mad-cow disease (Bovine Spongiform Encephalopathy or BSE) and Creutzfeldt-Jakob Disease (Griffith, 1967; Prusiner, 1982; Collinge, 1999). In the yeast *S. cerevisiae*, prion proteins such as Sup35 and Ure2 create heritable phenotypes, but unlike their mammalian counterparts these prions do not alter the viability of the organism (Tuite and Cox, 2009; Fowler and Kelly, 2009; Sindi and Serio, 2009).

According to the prion hypothesis, new phenotypes arise when abnormally folded versions of a protein appear (Figure 1a) and are joined together in aggregates. These aggregates are complexes of multiple abnormal proteins and range in size from tens to hundreds of proteins. The abnormal (prion) state is infectious and can spread to normal proteins within the cell by *converting* their conformation to the prion state.

*Communicated by Peter Jagers and Christine Jacob.

Address correspondence to Suzanne S. Sindi, School of Natural Sciences, University of California, Merced, 5200 Lake Rd., Merced, CA, 95343, USA. E-mail: ssindi@ucmerced.edu

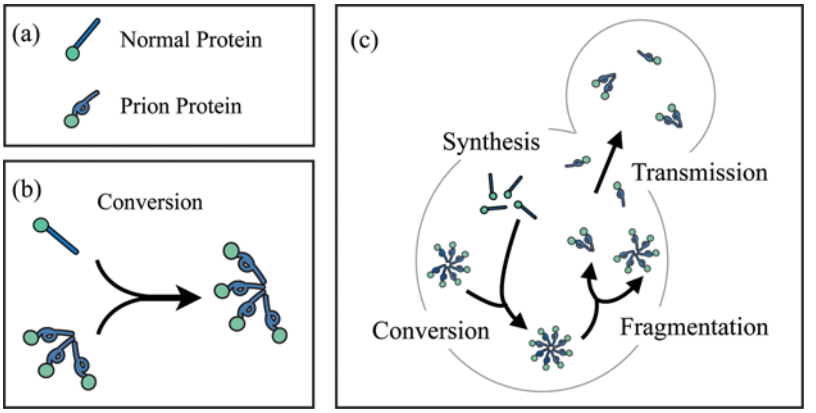


**Figure 1.** *Yeast Prion Cycle.* (a) A prion protein is capable of existing in either a normal or abnormal (prion) state. (b) Proteins in the prion state form aggregates which then induce conversion of the normal protein to the prion state. The resulting protein is incorporated into the existing aggregate. (c) Within a growing yeast culture, four steps are essential for the persistence of the prion state: *synthesis* of normal protein, *conversion* of normal protein by aggregates, *fragmentation* of aggregates into smaller complexes, and *transmission* of prion aggregates from mother to daughter cell. (Color figure available online.)

During this process, the newly modified protein joins the complex and the aggregate increases in size (Figure 1b).

Because cell divisions result in an exponentially growing total number of cells, in order for the prion proteins to be present throughout a colony, the total number of aggregates must increase. Four biochemical processes maintain the prion phenotype in a growing yeast culture (Figure 1c): (1) *synthesis* of new normal protein, (2) *conversion* of normal protein to the prion state by existing aggregates, (3) creation of new prion aggregates through *fragmentation* of existing aggregates into smaller complexes, and (4) *transmission* of a subset of prion aggregates through cell division.

Inducing loss of the prion phenotype by perturbing one of the steps in the prion cycle is a common method for experimental analysis of the prion process. For example, loss of the prion state has been used to investigate the total number of prion aggregates in a yeast cell. For the yeast prion protein Sup35, sufficiently high concentrations of guanidine hydrochloride (GdnHCl) have been shown to halt the fragmentation process (Byrne et al., 2007). Although synthesis and conversion continue normally, because no new prion aggregates are created, the existing aggregates are gradually diluted through cell division and the population is eventually *cured* of the prion state because the fraction of cells with prion aggregates decreases to zero.

Morgan et al. (2003) developed a novel way to estimate the total number of prion aggregates by studying cultures grown with the addition of GdnHCl. The authors estimated the total number of initial aggregates, $n_0$, in a cell by analyzing the rate of loss of the prion state as the population grows in the presence of GdnHCl. Morgan et al. (2003) modelled cell division as a binary fission process; that is, during cell division, prion aggregates are equally likely to end up in either resulting cell.

Cole et al. (2004) improved on Morgan et al. (2003) by incorporating two biologically relevant asymmetries in yeast cell division. First, a newly born daughter takes

longer to divide the first time than in subsequent divisions. Second, the volume difference between mature (mother) and newly born (daughter) cells suggests that daughter cells will inherit fewer than 50% of the aggregates. Cole et al. (2004) and Byrne et al. (2009) fixed parameters related to cell growth and estimated the total number of aggregates $n_0$ and the proportion $\pi$ transmitted to daughter cells from curing experiments.

Both Morgan et al. (2003) and Cole et al. (2004) assume all prion aggregates are equally transmissible. However Ghaemmaghami et al. (2007), Sindi and Serio (2009), Calvez et al. (2009), and Derdowski et al. (2010) suggest that only a subset of the aggregate population is capable of transmission. Derdowski et al. (2010) observed that for the yeast prion protein Sup35, only aggregates below a threshold size, about 20 monomers, can be efficiently transmitted during cell division. However, because aggregates may increase or decrease in size over time, the set of transmissible aggregates changes over time.

As the addition of GdnHCl at sufficiently high concentrations stops only the fragmentation process, aggregates will continue to grow through converting normal protein (Ness et al., 2002; Satpute-Krishnan et al., 2007). Over time, some aggregates become too large to transmit and remain in the mother cell. Cox et al. (2003) found that in the presence of GdnHCl, transmission of aggregates is biased toward retention in the mother cell and this bias increases over time; Palmer et al. (2011) attribute this bias to continued conversion. Without size-dependent transmission of prion aggregates, Cole et al. (2004) and Byrne et al. (2009) underestimate the total number of transmissible aggregates in the founding cell.

We develop a branching process to model loss of the prion state in a growing culture of yeast cells with continued aggregate growth and size-dependent aggregate transmission. Palmer et al. (2011) model size-based transmissibility but do not quantify loss of the prion state formally. Using a discrete-time model of cell division, we express the fraction of cells containing prion aggregates in a growing population. We use simulations to show that while prior models assuming equal transmissibility of aggregates describe loss of the prion state in time accurately, these models underestimate the total number of aggregates.

## 2. BRANCHING PROCESS MODEL

We model curing, loss of prion aggregates, in a population arising from a single cell with some initial total number of prion aggregates each with an associated size. In the discrete-time model, the population grows through nonoverlapping generations during which each individual cell divides, doubling the population at each iterate. Although we neglect asynchronous effects due to individual lifetime variation, the model is still a useful approximation, especially if the variability in individual lifetimes is low. We shall also point out the effect on estimation of the initial total number of prion aggregates when conversion is taken into account.

A given cell can be either a mother, M, if it has previously reproduced, or a daughter, D, if it has not reproduced yet. After each reproduction event, we consider the two resulting cells to be newborn, even though one of them actually is the mother. A mother gives birth to a mother and a daughter, and a daughter gives birth to a mother and a daughter as well. The importance of distinguishing between mothers and daughters comes from prion conversion.

We model conversion by having each prion aggregate independently growing in size, one unit at a time, according to a Poisson process with rate $\beta$ (Figure 1). We take the generation time to be unity, and therefore $\beta$ is the expected number of conversion events per aggregate per generation. Once a prion aggregate has grown to a critical size, it can no longer be transmitted to the daughter and is retained in the mother cell during division. When cells divide, aggregates smaller than the transmission threshold $T$ are transmitted to newly created daughter cells according to a binomial distribution with success probability $p$. Aggregates with size greater than or equal to $T$ remain in the mother cell.

In any given generation there will be cells with and without prion aggregates. Our goal is to get an expression for the expected proportion of cells with prions at a given time $t$, which is the type of data that can be assessed in curing experiments. We do not consider cell death. As a typical yeast cell survives for roughly 25 generations (Sinclair et al., 1998) and a curing experiment typically lasts less than 30 hours, or 20 generations, loss of the prion state due to cell death is negligible (Morgan et al., 2003; Cole et al., 2004).



### 2.1. Uniform Initial Aggregate Size

$Z_n$ is the total number of cells with prions in generation $n$, starting from an ancestor with $N_i$ prion aggregates which are $i$ units from reaching the critical size, at which point transmission to a daughter cell is no longer possible. The expected proportion of cells with prions in generation $n$ conditioned on $N_i$ is:

$$P_n^{(N_i)} = \frac{E(Z_n|N_i)}{2^n} \tag{1}$$

and the unconditional expected proportion:

$$P_n = \frac{E(Z_n)}{2^n}. \tag{2}$$

First, we find an expression for the conditional expectation $E(Z_n|N_i)$. Each cell in the $n$th generation is described by a sequence of mothers and daughters. Once a prion aggregate reaches critical size, it cannot be transmitted to the daughter but must stay in the mother; thus, we divide the set of the $2^n$ possible sequences of mothers and daughters into subsets $S_{nld}$ of sequences where the last daughter is in position $l$ and where there are a total of $d$ daughters. For example, the sequence DDMMM is in $S_{522}$, the sequences DMDMM and MDDMM are both in $S_{532}$, and so on. Let $n_{ld}$ be the total number of sequences in $S_{nld}$; then $n_{ld} = \binom{l-1}{d-1}$ for $l = 0, \ldots, n$ and $d = 0, \ldots, l$, where $\binom{-1}{-1} = 1$ and $\binom{l-1}{-1} = 0$ for $l \geq 1$. The total number $n_{ld}$ does not depend on $n$ because after the final daughter there are no further choices. For fixed $n$, the $n_{ld}$ sum to $2^n$.

$A_n$ is the event that a cell has prions in the $n$th generation and $P_{ld}^{(r)}$ denotes the probability measure for a sequence in $S_{nld}$ given that the initial total number of prion aggregates is $r$. We have

$$E(Z_n|N_i) = \sum_{l=0}^{n} \sum_{d=0}^{l} \binom{l-1}{d-1} P_{ld}^{(N_i)}(A_n). \tag{3}$$

Because aggregates are transmitted independently of each other, we get:

$$P_{ld}^{(N_i)}(A_n) = 1 - \left(1 - P_{ld}^{(1)}(A_n)\right)^{N_i}, \tag{4}$$

where $1 - P_{ld}^{(1)}(A_n)$ is the probability that a given prion aggregate in the ancestor does not appear in the $n$th generation, in the given sequence. If $N_i$ has probability generating function (pgf) $\varphi$, given by

$$\varphi(s) = E(s^{N_i}), \tag{5}$$

the unconditional probability is:

$$P_{ld}(A_n) = E\left(P_{ld}^{(N_i)}(A_n)\right) = 1 - E\left(\left(1 - P_{ld}^{(1)}(A_n)\right)^{N_i}\right) = 1 - \varphi\left(1 - P_{ld}^{(1)}(A_n)\right) \tag{6}$$

so that

$$E(Z_n) = \sum_{l=0}^{n}\sum_{d=0}^{l}\binom{l-1}{d-1}\left(1 - \varphi\left(1 - P_{ld}^{(1)}(A_n)\right)\right). \tag{7}$$

To obtain an expression for $P_{ld}^{(1)}(A_n)$, we condition on the critical generation $G$, which is the generation in which the aggregate reaches its critical size and is no longer transmissible to daughters. What is important here is that $l$ is the position for the final daughter, so from $l+1$ on, the sequence consists of only mother cells. If $G < l$, the aggregate cannot be present in the sequence because it cannot be passed on to the final daughter cell; hence, the probability is positive only for $G \geq l$. Specifically, if $G = j$ where $l \leq j < n$, the prion aggregate must successfully reach generation $j$ by chance, after which it stays in the mother cell. Let $p$ be the probability that the aggregate is passed on to the daughter so that $1 - p$ is the probability it stays in the mother. We then get:

$$P_{ld}^{(1)}(A_n | G = j) = p^d(1-p)^{j-d} \tag{8}$$

for $l = 0, \ldots, n$ and $d = 0, \ldots, l$ which gives:

$$P_{ld}^{(1)}(A_n) = \sum_{j=l}^{n-1} p^d(1-p)^{j-d}P_i(G = j) + p^d(1-p)^{n-d}P_i(G \geq n). \tag{9}$$

Before the first generation, $n = 0$ which implies $l = d = 0$ and gives $P_{00}^{(1)}(A_0) = 1$ as expected. The notation $P_i$ indicates that the distribution of $G$ depends on $i$, the remaining number of conversion events until the critical size is reached. The expression (2) for the expected fraction of cells with prions in generation $n$ is given by:

**Proposition 1.**

$$P_n = 2^{-n}\left(\sum_{l=0}^{n}\sum_{d=0}^{l}\binom{l-1}{d-1}\left(1 - \varphi\left(1 - P_{ld}^{(1)}(A_n)\right)\right)\right), \tag{10}$$

*where $\varphi$ is the pgf of the initial total number of prion aggregates, $N_i$, and the $P_{ld}^{(1)}(A_n)$ are given by Eq. (9).*

Because prion conversion is a Poisson process with rate $\beta$, the times between successive conversion events are independent random variables having the exponential distribution with rate $\beta$ (mean $1/\beta$). Denoting their common distribution function by $H$, the probabilities $P_i(G=j)$ appearing in Eq. (9), are given by:

$$P_i(G=j) = H^{*i}(j+1) - H^{*i}(j), \tag{11}$$

where $*$ denotes convolution. $H^{*i}$ is the distribution function for the gamma distribution with parameters $i$ and $\beta$. For $j=0$ we get:

$$P_i(G=0) = H^{*i}(1), \tag{12}$$

the probability that there are at least $i$ conversion events before the ancestor divides.

In the special case $N_i \sim \text{Poi}(n_i)$, a Poisson distribution with mean $n_i$, we have $\varphi(s) = \exp(n_i(s-1))$ which gives

$$P_n = 2^{-n} \sum_{l=0}^{n} \sum_{d=0}^{l} \binom{l-1}{d-1} \left(1 - \exp\left(-n_i P_{ld}^{(1)}(A_n)\right)\right). \tag{13}$$

### 2.2. Many Initial Aggregate Sizes

We generalize the model by introducing $m$ different initial aggregate sizes. The initial cell contains $N_i$ prion aggregates which are $i$ units away from the critical size for $i=1, 2, \ldots, m$. In a slight generalization from the previous section, $P_{ld}^{(N_1,\ldots,N_m)}$ is the probability measure for a sequence in $S_{ld}$ given these initial conditions, and $P_{ld}^{(1,i)}$ is the probability measure for a sequence in $S_{ld}$ for one initial prion aggregate $i$ units away from the critical size. The analog of Eq. (4) is:

$$P_{ld}^{(N_1,\ldots,N_m)}(A_n) = 1 - \prod_{i=1}^{m} \left(1 - P_{ld}^{(1,i)}(A_n)\right)^{N_i}, \tag{14}$$

which gives the unconditional probability

$$P_{ld}(A_n) = 1 - \varphi\left(1 - P_{ld}^{(1,1)}(A_n), 1 - P_{ld}^{(1,2)}(A_n), \ldots, 1 - P_{ld}^{(1,m)}(A_n)\right), \tag{15}$$

where $\varphi$ now denotes the joint pgf of the random vector $(N_1, N_2, \ldots, N_m)$. With this adjustment, the expression for $P_n$ given in Proposition 1 remains the same. Although in practice the initial aggregate distribution is likely to be tightly controlled by parameters governing the full prion pathway (Masel et al., 1999; Greer et al., 2006), if the $N_i$ are independent, the pgf factors into the product of the individual pgfs. In particular, if the $N_i$ are independent with $N_i \sim \text{Poi}(n_i)$, we get:

$$P_{ld}(A_n) = 1 - \exp\left(-\sum_{i=1}^{m} n_i P_{ld}^{(1,i)}(A_n)\right), \tag{16}$$

which corresponds to

$$P_n = 2^{-n} \sum_{l=0}^{n} \sum_{d=0}^{l} \binom{l-1}{d-1} \left(1 - \exp\left(-\sum_{i=1}^{m} n_i P_{ld}^{(1,i)}(A_n)\right)\right). \tag{17}$$

The $P_{ld}^{(1,i)}$ are computed as in Eq. (9), substituting $P_{ld}^{(1,i)}$ for $P_{ld}^{(1)}$, using the dependence on $i$ of the distribution of $G$.

## 3. SIMULATIONS

We simulate yeast populations founded by a single cell with some initial complement of aggregates under synchronous cell division. We show that models of prion curing neglecting continued conversion and size-dependent transmission produce curing curves which closely match those from our model but which underestimate the total number of prion aggregates in the initial cell. We give some insight into practical limitations in estimating model parameters from the curing data directly. Similar difficulties in parameter estimation were previously reported by Palmer et al. (2011).

### 3.1. Uniform Initial Aggregate Size

All aggregates in the founder cell at generation $n = 0$ have the same size, $i$ units away from the transmission threshold. During a cell's lifetime, prion aggregates grow according to a Poisson process with rate $\beta$. Cells divide synchronously at each unit time, during division aggregates smaller than the transmission threshold are retained in the mother cell, while other aggregates are transmitted to the daughter with probability $p = 0.40$. We fix $p = 0.40$, the value established by Morgan et al. (2003), Cole et al. (2004), and Palmer et al. (2011).

In Figure 2, we compare our theoretical result, Eq. (13), to simulations of curing for three different regimes of $\beta$: fast, medium, and slow prion growth. In each simulation, the population begins with a single cell with a Poisson distributed total number of initial aggregates, with mean $n_0 = 200$ and $i = 20$. All aggregates are 20 conversions away from the transmission threshold. We plot our theoretical curing curve along with the 5th and 95th percentiles from 100 independent simulations. Our theoretical curves agree with the simulations over all rates of conversion.

Depending on the rate of aggregate growth, loss of prion aggregates in the population is caused by distinct mechanisms. When conversion is much faster than cell division, with high probability all aggregates reach critical size before the initial cell divides. The rate of curing is simply the rate of exponential population growth (Figure 2a). When conversion is much slower than cell division, aggregates remain transmissible for longer and the rate of loss is dominated by dilution of aggregates in cell division. The rate of loss of the prion state in Figure 2(c) is slower than that in Figures 2(a) and 2(b). For intermediate rates of growth, Figure 2(b), loss of the prion state becomes a combination of dilution of aggregates due to exponential population growth and eventually the transmission deficiency from larger aggregates.

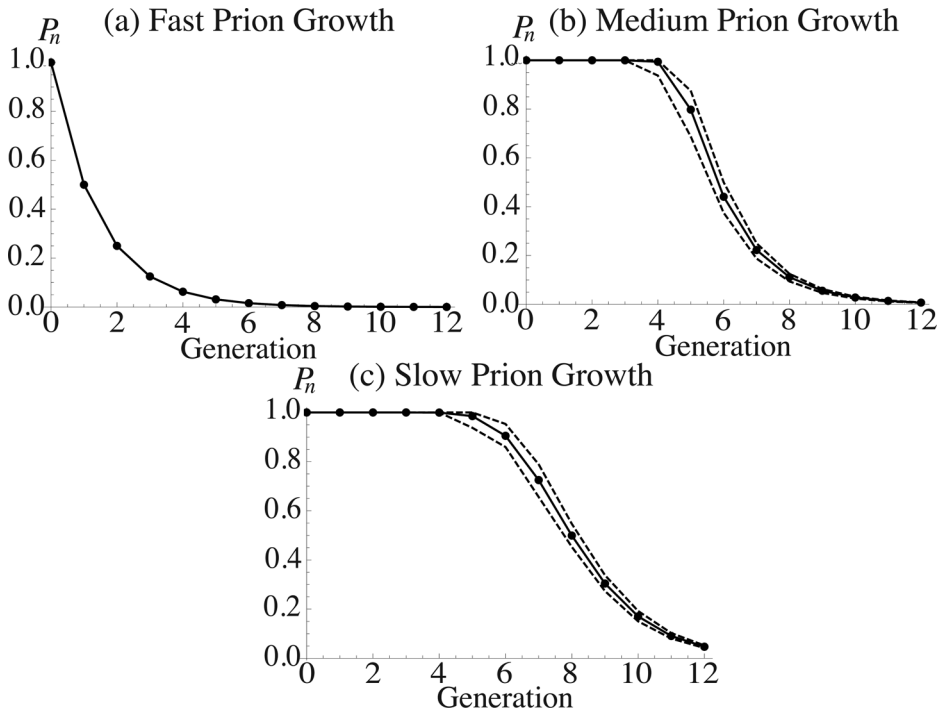


**Figure 2.** Our derived results agree with simulations for three distinct regimes of prion growth: fast, medium, and slow. In addition to our theoretical distribution (dotted curve) we plot the 5th and 95th percentiles (dashed curves) from 100 independent simulations.

### 3.2. Many Initial Aggregate Sizes

To study the effect of loss when the founder cell has aggregates of multiple initial sizes, we simulate populations where the founder cell has two sizes of initial aggregates, $i_1$ and $i_2$, units away from the transmission threshold. The initial total number of aggregates of each size is independently drawn from a Poisson distribution with the same mean $n_0$.

When the variance in aggregate sizes is small, Eq. (13) describes loss. However, when the variance of initial aggregate sizes is large, the generalized Eq. (17) is needed to depict the curing process. In Figure 3, we show the 5th and 95th percentiles from 100 simulations where the founding cell has an average of 100 aggregates that are 10 conversions away from $T$ ($i_1 = 10$, $n_0 = 100$) and 100 aggregates that are 40 conversions from $T$ ($i_2 = 40$, $n_0 = 100$) all with the same rate of conversion $\beta = 0.21$.

As shown in Figure 3(a), our theoretical curve, Eq. (17), matches the simulations. In contrast, considering only the average initial aggregate size, Eq. (13), results in deviations from the simulations (Figure 3b). By considering only the average aggregate size we underestimate early loss, because aggregates become too large to transmit sooner than predicted by the average size, and overestimate later loss, because aggregates remain transmissible longer than predicted by the average size.

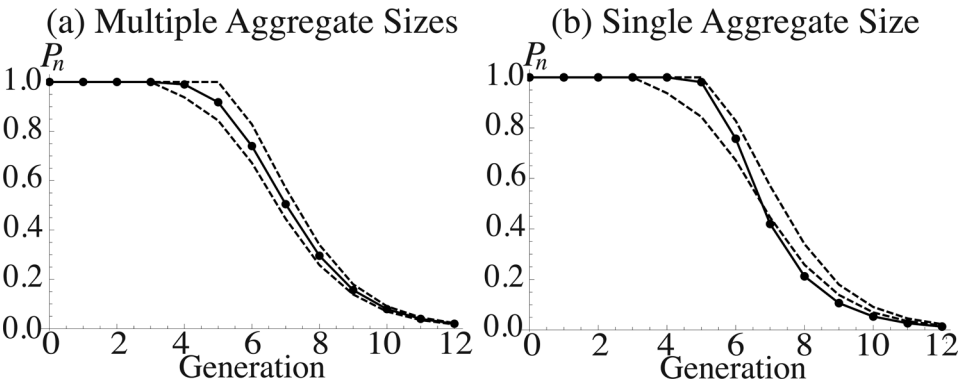


**Figure 3.** Accuracy of our mode of prion loss when the founding cell has aggregates with two different initial sizes, $i_1 = 10$, $i_2 = 40$, with $\beta = 0.21$, and $n_0 = 100$ for both sizes. Eq. (17) with multiple initial aggregate sizes (a) describes the data more accurately than Eq. (13) where the average initial aggregate size is used (b).

### 3.3. Neglecting Conversion and Size-Dependent Transmission Underestimates the Total Number of Prion Aggregates

Morgan et al. (2003) and Cole et al. (2004) assumed all aggregates to be equally transmissible at all times and that the appearance of loss during a curing experiment comes only from dilution of aggregates by cell division, with no effect from retention of larger aggregates in mother cells. When the rate of aggregate conversion is much slower than the rate of cell division, loss is not affected by conversion and, as such, estimating the total number of prion aggregates using these models should closely match the true number. However, when aggregates become too large to transmit before the population grows large enough fully to dilute the aggregates, such models will underestimate the total number of initial aggregates.

When aggregates of all sizes are transmissible, the probability of having aggregates in a cell at generation $n$ is purely a function of the binomial probability of transmission. Eq. (9) greatly simplifies because we need not distinguish between different sequences in $S_{nld}$:

$$P_{ld}^{(1)}(A_n) = p^d(1-p)^{(n-d)}. \tag{18}$$

Applying Proposition 1 and simplifying yields the expected fraction of cells with prion aggregates in generation $n$:

$$P_n = 1 - 2^{-n}\exp(-n_0)\sum_{d=0}^{n}\binom{n}{d}\exp(p^d(1-p)^{n-d}). \tag{19}$$

Figure 4 shows theoretical curing curves from our model, $\beta = 0.37$, $i = 20$ and $p = 0.40$, (dotted curve) along with estimated curing curves assuming aggregates of all sizes are transmissible (dashed curve with squares). We estimate the parameter $n_0$ by minimizing the least-squared error between Eq. (19) and (13) with $\beta = 0.37$

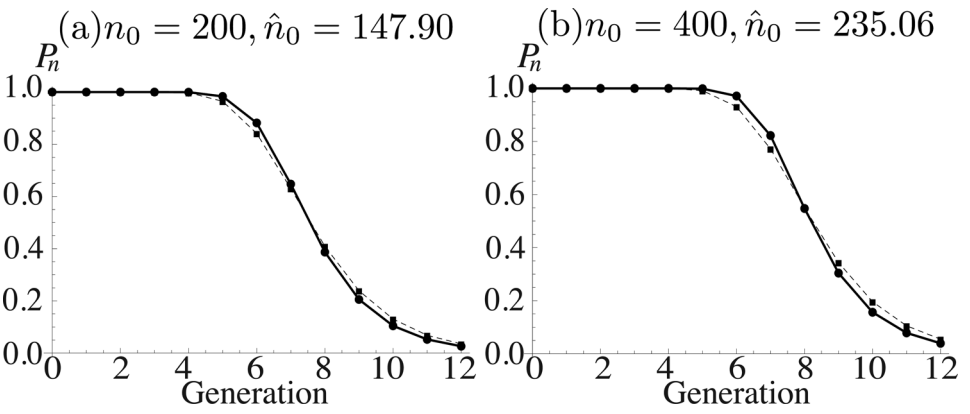


**Figure 4.** Models of prion curing curves neglecting conversion and size-dependent transmission underestimate the initial number of aggregates, and this deviation increases with increasing $n_0$ for a fixed conversion rate $\beta$. In (a) and (b) we plot curves from the fixed-size model (Eq. (13)) (dotted curve) and their least-squared approximations from an analogous model assuming all aggregates are equally transmissible (Eq. (19)) (dashed curve with squares). Although a model neglecting size-dependent transmission can produce very similar curing curves, the total number of aggregates is underestimated by 25% in (a) and 40% in (b).

and $i = 20$. Although the model without conversion (Eq. (19)) produces similar curing curves to those produced by our model (least squared error $\leq 0.09$), the model without conversion underestimates the total number of aggregates by 25% when $n_0 = 200 (\hat{n}_0 = 147.89)$ and 40% when $n_0 = 400 (\hat{n}_0 = 235.06)$.

For a fixed conversion rate $\beta$, we expect the deviation in estimating $n_0$ with Eq. (19) to increase with the true total number of initial aggregates. The increased deviation arises from the fact that as the total number of aggregates increases, the minimum observed critical generation decreases. The more aggregates present, the more likely that some aggregates will become too large to transmit by a given generation $n$. The deviation between the true $n_0$ and the estimate for $n_0$ obtained from Eq. (19) also increases with increasing conversion rate $\beta$ and decreasing $i$ as both factors decrease the number of generations in which an aggregate remains transmissible.

### 3.4. Complications in Estimating Parameters From Curing Experiments

Although Eq. (13) models loss of the prion state more accurately than previous models neglecting the effects of conversion, difficulties arise when attempting to estimate parameters from data. Because aggregates larger than the threshold size cannot be transmitted, many aggregates growing quickly can look like fewer aggregates growing more slowly. Prior knowledge of parameters is likely to be essential when analyzing experimental data.

To illustrate the similarity between solutions of Eq. (13), Figure 5 shows two solutions corresponding to very different numbers of initial aggregates, $n_0 = 200$ and $n_0 = 372$. The similarity between these solutions comes from the relationship between conversion rate and initial aggregate size. In the case with fewer aggregates, the conversion rate is lower ($\beta = 0.37$ compared to $\beta = 1$) and the initial aggregate size is farther from the transmission threshold (20 units versus 6 units). Two hundred

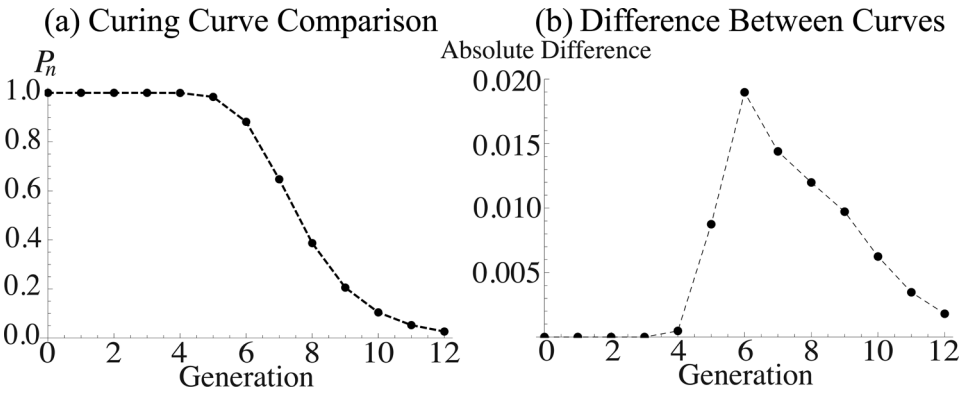


**Figure 5.** Similarity in curing curves for different parameters: (a) two theoretical curing curves and (b) their absolute differences. In (a) we show curing curves for different parameter values, (dots alone) $\beta = 0.37$, $n_0 = 200$, and $i = 20$ with (dashed curve) $\beta = 1$, $n_0 = 372$, and $i = 6$. The two curing curves are similar, with least squares difference of $\approx 0.01$.

aggregates with the slower growth rate dilute through the population in a nearly identical fashion to the 372 aggregates with a faster growth rate.

The correlation among $n_0$, $\beta$, and the initial aggregate size is reflected by the log-least-squares deviation between three simulated curing curves, generated with

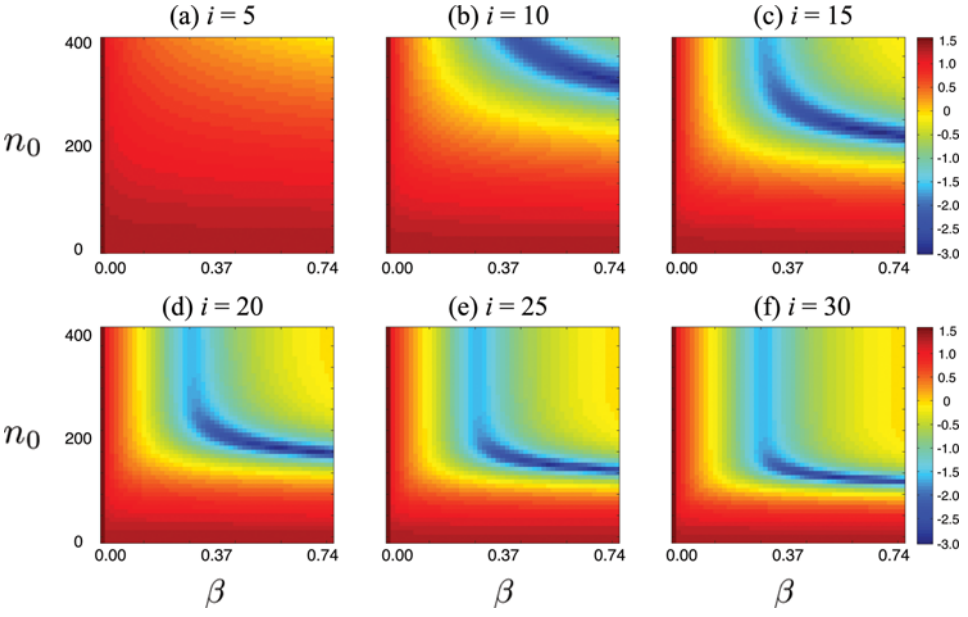


**Figure 6.** Log-least-squares error of three simulated curing curves ($n_0 = 200$, $\beta = 0.36$, and $i = 20$) compared with Eq. (13) for $10^{-6} \leq \beta \leq 0.74$, $0 \leq n_0 \leq 400$, and different initial prion sizes $i$. The true parameters used to generate the simulated curing curves lie in the center of Figure 6(d). There is a trade-off between many aggregates growing slowly and fewer growing faster. Multiple parameter combinations yield highly similar curing curves. (Color figure available online.)

$n_0 = 200$, $i = 20$, $\beta = 0.37$, and solutions to Eq. (13) over a wide range of parameters. In Figures 6(a)–(f) for a fixed choice of $i$ ($5 \leq i \leq 30$) we vary $n_0$ and $\beta$ ($0 \leq n_0 \leq 400$, $10^{-6} \leq \beta \leq 0.74$) and plot the log-least-squared difference of Eq. (13) from the simulations. The parameters used to generate the simulations lie in the center of Figure 6d. These figures illustrate the dependency between $n_0$ and $\beta$ with respect to the trade-off between many aggregates growing slowly and fewer aggregates growing quickly. In particular, for any choice of $i$, combinations of $n_0$ and $\beta$ have log-least-squares difference close to optimal.

In addition to the specific example in Figure 6, there are a number of other cases for which solutions to Eq. (13) are nearly identical. For example, when the expected time for an aggregate to exceed the transmission threshold is large enough that aggregates are likely to have diluted to a single aggregate per cell, solutions to Eq. (13) with smaller conversion rate or initial size yield nearly identical curing curves. The similarity of curing curves for distinct parameter combinations means that prior knowledge is important when seeking to estimate parameters from data. In addition, rather than seeking the unique set of parameters minimizing error between the theoretical curing curve and experimental observations, we may constrain the parameters by fixing the expected critical generation, which depends on the ratio of $i$ and $\beta$.

## 4. CONCLUSION

We expressed theoretical curing curves based on the assumption of discrete-time division and that prion aggregates exceeding a threshold size are no longer transmissible. We estimated the total number of transmissible aggregates in the founding cell, when other parameters are known. By neglecting conversion and transmission deficiencies, previous models underestimate this number. We provide the first model amenable to estimating the rate of conversion from curing experiments. Previously, estimates of the rate of conversion were based on the analysis of *in vitro* experiments (Tanaka et al., 2006; Palmer et al., 2011).

We considered the transmission of prion aggregates to be constrained by a threshold where aggregates exceeding the threshold are always retained by the mother cell. However, the true mechanism may be more subtle with a decreasing probability of transmission as aggregate size increases (Derdowski et al., 2010; Palmer et al., 2011).

## ACKNOWLEDGMENTS

The work was supported by NIH grant 1R15GM093957-01 to Peter Oloffson and NIH grant 1F32GM089049-01 to Suzanne S. Sindi.

## REFERENCES

Byrne, L.J., Cole, D.J., and Cox, B.S., et al. (2009). The number and transmission of [*PSI*$^+$] prion seeds (propagons) in the yeast *Saccharomyces cerevisiae*. *PLoS ONE*, *4*(3): e4670.

Byrne, L.J., Cox, B.S., and Cole, D.J., et al. (2007). Cell division is essential for elimination of the yeast [*PSI*$^+$] prion by guanidine hydrochloride. *Proceedings of the National Academy of Sciences*, *104*(28): 11688–11693.

Calvez, V., Lenuzza, N., and Oelz, D., et al. (2009). Size distribution dependence of prion aggregates infectivity. *Mathematical Biosciences*, *217*(1): 88–99.

Cole, D.J., Morgan, B.J.T., and Ridout, M.S., et al. (2004). Estimating the number of prions in yeast cells. *Mathematical Medicine and Biology*, *21*(4): 369–395.

Collinge, J. (1999). Variant Creutzfeldt-Jakob disease. *The Lancet*, *354*: 317–323.

Cox, B., Ness, F., and Tuite, M. (2003). Analysis of the generation and segregation of propagons: Entities that propagate the [$PSI^+$] prion in yeast. *Genetics*, *165*(1): 23–33.

Derdowski, A., Sindi, S., and Klaips, C., et al. (2010). A size threshold limits prion transmission and establishes phenotypic diversity. *Science*, *330*(6004): 680–683.

Fowler, D.M. and Kelly, J.W. (2009). Aggregating knowledge about prions and amyloid. *Cell*, *137*(1): 20–22.

Ghaemmaghami, S., Phuan, P.W., and Perkins, B., et al. (2007). Cell division modulates prion accumulation in cultured cells. *Proceedings of the National Academy of Sciences*, *104*(46): 17971–17976.

Greer, M.L., Pujo-Menjouet, L., and Webb, G.F. (2006). A mathematical analysis of the dynamics of prion proliferation. *Journal of Theoretical Biology*, *242*(3): 598–606.

Griffith, J.S. (1967). Self-replication and scrapie. *Nature*, *215*(5105): 1043–1044.

Masel, J., Jansen, V.A.A., and Nowak, M.A. (1999). Quantifying the kinetic parameters of prion replication. *Biophysical Chemistry*, *77*(2–3): 139–152.

Morgan, B.J.T., Ridout, M.S., and Ruddock, L.W. (2003). Models for yeast prions. *Biometrics*, *59*(3): 562–569.

Ness, F., Ferreira, P., and Cox, B., et al. (2002). Guanidine hydrochloride inhibits the generation of prion "Seeds" but not prion protein aggregation in yeast. *Molecular and cellular biology*, *22*(15): 5593–5605.

Palmer, K.J., Ridout, M.S., and Morgan, B.J.T. (2011). Kinetic models of guanidine hydrochloride-induced curing of the yeast [$PSI^+$] prion. *Journal of Theoretical Biology*, *274*(1): 1–11.

Prusiner, S. (1982). Novel proteinaceous infectious particles cause scrapie. *Science*, *216*(4542): 136–144.

Satpute-Krishnan, P., Langseth, S.X., and Serio, T.R. (2007). Hsp104-Dependent remodeling of prion complexes mediates protein-only inheritance. *PLoS Biology*, *5*(2): e24.

Sinclair, D., Mills, K., and Guarente, L. (1998). Aging in *Saccharomyces cerevisiae*. *Annual Reviews in Microbiology*, *52*(1): 533–560.

Sindi, S.S. and Serio, T.R. (2009). Prion dynamics and the quest for the genetic determinant in Protein-only inheritance. *Current Opinion in Microbiology*, *12*(6): 623–630.

Tanaka, M., Collins, S.R., and Toyama, B.H., et al. (2006). The physical basis of how prion conformations determine strain phenotypes. *Nature*, *442*(7102): 585–589.

Tuite, M.F. and Cox, B.S. (2009). Prions remodel gene expression in yeast. *Nature Cell Biology*, *11*(3): 241–243.